

Z-peaked excess in goldstini scenarios

Seng Pei Liew^a, Alberto Mariotti^b, Kentarou Mawatari^b, Kazuki Sakurai^c, Matthias Vereecken^b

^a*Department of Physics, University of Tokyo, Bunkyo-ku, Tokyo 113-0033, Japan*

^b*Theoretische Natuurkunde and IIHE/ELEM, Vrije Universiteit Brussel, and International Solvay Institutes, Pleinlaan 2, B-1050 Brussels, Belgium*

^c*Department of Physics, King's College London, London WC2R 2LS, UK*

Abstract

We study a possible explanation of a 3.0σ excess recently reported by the ATLAS Collaboration in events with Z -peaked same-flavour opposite-sign lepton pair, jets and large missing transverse momentum in the context of gauge-mediated SUSY breaking with more than one hidden sector, the so-called goldstini scenario. In a certain parameter space, the gluino two-body decay chain $\tilde{g} \rightarrow g\tilde{\chi}_{1,2}^0 \rightarrow gZ\tilde{G}'$ becomes dominant, where $\tilde{\chi}_{1,2}^0$ and \tilde{G}' are the Higgsino-like neutralino and the massive pseudo-goldstino, respectively, and gluino pair production can contribute to the signal. We find that a mass spectrum such as $m_{\tilde{g}} \sim 1000$ GeV, $m_{\tilde{\chi}_{1,2}^0} \sim 800$ GeV and $m_{\tilde{G}'} \sim 600$ GeV demonstrates the rate and the distributions of the excess, without conflicting with the stringent constraints from jets plus missing energy analyses and with the CMS constraint on the identical final state.

1. Introduction

While the LHC Run-I achieved a great success with the discovery of the Higgs boson, most of the attempts to find new physics failed, and hence we are eagerly waiting for results from the LHC Run-II, which has just started and entered a new energy frontier.

However, although no significant signs for new physics at the 7 and 8 TeV run have been reported so far, we should still keep our eye on the possible faintest imprint. The ATLAS Collaboration has recently reported a search for supersymmetry (SUSY) with the final state containing a pair of same-flavour opposite-sign (SFOS) leptons, jets and large missing transverse momentum (\cancel{E}_T) at a centre-of-mass energy of 8 TeV [1]. With data for an integrated luminosity of 20.3 fb^{-1} , an intriguing excess of 29 lepton pairs peaked at the invariant mass of the Z boson (“on- Z ”) is observed, while 10.6 ± 3.2 pairs are expected from the Standard Model (SM) prediction. The excess corresponds to a significance of 3.0σ .

Interpretation of the excess with some models is not a straightforward task, as null results from other searches are placing considerably stringent constraints on the viable model parameter space. The ATLAS on- Z signal region is motivated by search for a pair production of gluino in gauge mediation scenarios in the minimal supersymmetric standard model (MSSM), where gluino decays into a neutralino, which subsequently decays into a Z boson accompanied by a very light gravitino. The gravitino escapes detection, leading to missing momentum. While relatively light gluinos with $m_{\tilde{g}} < 1.2$ TeV are required [2],

studies presented in [3, 4] have shown that explaining the excess within this scenario is difficult. At large gluino–neutralino mass splitting, gluino decays with a significant branching ratio into a top quark, leading to appreciably strong bounds from the stop searches. Even in the compressed gluino–neutralino mass region, the process with the hadronic decay mode of the energetic Z boson is constrained by the dedicated jets plus \cancel{E}_T searches. Given that situation, several solutions have been proposed in various models, e.g. NMSSM [3, 5], MSSM with a light sbottom or stop [6], pMSSM [7], split SUSY [8], as well as non-SUSY models [9, 10].

In this paper, we investigate an alternative SUSY model, i.e. a model with multiple hidden sectors, the so-called goldstini model [11–14], especially in the context of gauge mediated SUSY breaking. We consider a gluino (\tilde{g}), the lightest and second lightest neutralinos ($\tilde{\chi}_{1,2}^0$), and a pseudo-goldstino (\tilde{G}') in the spectrum as a simplified model. As we verify below, in a certain parameter space, the gluino two-body decay chain

$$\tilde{g} \rightarrow g + \tilde{\chi}_{1,2}^0 \rightarrow g + Z + \tilde{G}' \quad (1)$$

becomes dominant, and gluino pair production can contribute to the signal. Jets from the gluino decay and the hadronic Z decay are softened when the mass spectrum is compressed due to the massive nature of the pseudo-goldstino. We find that there is a viable parameter space even after the multijet plus \cancel{E}_T constraint [15], as well as the CMS constraint on the identical final state [16], are taken into account. We also show that the two-body gluino decay in (1) provides a better fit to the data for the distributions with respect to the three-body gluino decay $\tilde{g} \rightarrow q\bar{q}\tilde{\chi}_{1,2}^0$.

Email address: kentarou.mawatari@vub.ac.be (Kentarou Mawatari)

The paper is organized as follows: In Sec. 2, we briefly review the model involving two SUSY breaking sectors, and verify the gluino two-body decay chain in (1). In Sec. 3, we recast the ATLAS on- Z analysis for our benchmark scenarios to find a viable parameter space. The constraints coming from other searches are also discussed. Sec. 4 is devoted to our summary. In Appendix A we give the explicit formulas for the neutralino decays, while in Appendix B we present the validation of the implementation for the analyses.

2. Model

The model we consider, in order to explain the ATLAS Z -peaked excess, is a scenario of gauge mediation with more than one secluded SUSY breaking sector. Each SUSY breaking sector contains a massless goldstino, i.e. the goldstone fermion of spontaneous SUSY breaking. In a two-sector scenario there are then two massless goldstini. Models of goldstini have been studied in [11–14, 17–20, 20–25], and the description of goldstini in gauge mediation models and the quantum corrections to the pseudo-goldstino mass have been investigated in [14]. Indeed, when taking into account the mediation mechanism and the interaction of the SUSY breaking sector with the MSSM, a linear combination of the goldstini becomes the true goldstino (the longitudinal component of the gravitino), while the orthogonal combination is a pseudo-goldstino. Denoting with f_a and \tilde{G}_a the SUSY breaking scales and the goldstini of the two sectors respectively, the true (massless) goldstino and the pseudo-goldstino are

$$\tilde{G} = \frac{1}{F}(f_1\tilde{G}_1 + f_2\tilde{G}_2), \quad \tilde{G}' = \frac{1}{F}(-f_2\tilde{G}_1 + f_1\tilde{G}_2), \quad (2)$$

where $F = \sqrt{f_1^2 + f_2^2}$ is the total SUSY breaking scale. The true goldstino (or gravitino) mass is related to the SUSY breaking scale and the Planck scale as $m_{\tilde{G}} \propto F/M_{\text{Pl}}$, and hence the low-energy SUSY breaking scenario as in gauge mediation leads to a very light goldstino. On the other hand, the mass of the pseudo-goldstino is not protected by any symmetry and generically receives relevant quantum corrections, proportional to the SUSY breaking terms [14]. In our paper, we consider the pseudo-goldstino mass to be of the order of a few hundreds of GeV.

The interaction of each of the goldstini with the particles in the visible sector are determined by the supercurrent, and hence the couplings of the true goldstino and of the pseudo-goldstino with the MSSM states are also fixed in terms of the soft SUSY breaking masses. The noteworthy feature is that the pseudo-goldstino couplings are generically different with respect to the goldstino couplings. Indeed they depend on the relative contribution to the soft masses from each of the SUSY breaking sector, and they can be enhanced without changing the overall soft masses. This implies that the decay of SUSY particles can be dominantly into a massive pseudo-goldstino plus a SM

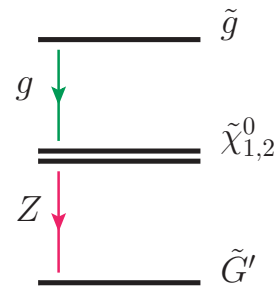


Figure 1: Mass spectrum for our simplified goldstini model, with the relevant decay modes.

particle, drastically changing the final state topology with respect to the usual decay into the true goldstino [20–25].

In this paper we consider a simplified model including as low energy degrees of freedom only a gluino, Higgsino-like neutralinos, a pseudo-goldstino and a goldstino. The mass spectrum of the model is depicted in Fig. 1. Note that the Higgsino fields include two almost degenerate neutral mass eigenstates and a charged one. We also note that the true goldstino is in the bottom of the spectrum, but is not shown in Fig. 1 since it is irrelevant in our scenario. In the following we study each decay step in detail to verify the gluino decay chain in (1).

Gluino decay. In the spectrum presented in Fig. 1 the gluino can potentially have several decay channels, depending on the mass splitting between the gluino and the neutralinos.

In case of the large splitting such as $(m_{\tilde{g}} - m_{\tilde{\chi}_i^0}) \gg m_t$, the tree-level three-body decays into a pair of third-generation quarks and a chargino/neutralino are dominant [4].

On the other hand, in the regime

$$\Delta m_{\tilde{g}-\tilde{\chi}_{1,2}^0} \equiv m_{\tilde{g}} - m_{\tilde{\chi}_{1,2}^0} \leq 200 \text{ GeV}, \quad (3)$$

the gluino decays predominantly into a gluon and a neutralino via a (s)top loop. The analytic expression for the $\tilde{g} \rightarrow g\tilde{\chi}_i^0$ decay can be found in [26, 27]. We find that this result is robust as soon as the Bino (M_B) and Wino (M_W) masses are moderately larger than the Higgsino mass (μ). We checked this decay pattern with SUSY-HIT [28], for instance, by fixing $m_{\tilde{g}} = 1000$ GeV, $\mu = 800$ GeV, and $\tan\beta = 10$, we find $B(\tilde{g} \rightarrow g\tilde{\chi}_{1,2}^0) > 85\%$ as soon as M_B and M_W are larger than about 1.4 TeV, with squark masses of the order $\mathcal{O}(5)$ TeV.

The gluino decays into a pseudo-goldstino or a goldstino with a gluon is also possible. However, unless the gluino coupling to the pseudo-goldstino is largely enhanced, these decay modes are always suppressed compared with the decays into the MSSM states.

In this paper, to fit the ATLAS excess, we consider the small mass splitting in Eq. (3), where the only $\tilde{g} \rightarrow g\tilde{\chi}_{1,2}^0$ decay is relevant.

Neutralino decay. The interaction lagrangian which is relevant for the neutralino decay into a pseudo-goldstino and an electroweak gauge boson or a Higgs boson is given by [11, 19, 21–23]

$$\begin{aligned} \mathcal{L}_{\tilde{G}'}^{\text{int}} = & i \frac{\tilde{y}_\gamma^i}{2\sqrt{2}F} \tilde{G}' \sigma^\mu \bar{\sigma}^\nu \tilde{\chi}_i^0 A_{\mu\nu} + i \frac{\tilde{y}_{Z_T}^i}{2\sqrt{2}F} \tilde{G}' \sigma^\mu \bar{\sigma}^\nu \tilde{\chi}_i^0 Z_{\mu\nu} \\ & + \frac{\tilde{y}_{Z_L}^i m_Z}{\sqrt{2}F} \tilde{\chi}_i^0 \bar{\sigma}^\mu \tilde{G}' Z_\mu + \frac{\tilde{y}_h^i}{\sqrt{2}F} \tilde{\chi}_i^0 \tilde{G}' h + h.c., \quad (4) \end{aligned}$$

where $A_{\mu\nu}$ and $Z_{\mu\nu}$ are the field strengths of the photon and the Z boson, respectively, and h is the lightest Higgs boson in the decoupling limit. The goldstino lagrangian is the same, but with different coefficients, $\tilde{y} \rightarrow y$. As mentioned above, the pseudo-goldstino couplings \tilde{y} can be larger than the goldstino couplings y , and in a simplified model approach they can be considered as free parameters [21, 22, 24]. Given a set of soft terms originating from the two SUSY breaking sectors, one can compute these couplings with the formulas collected in Appendix A.

Although the neutralino decay can present a rich pattern, with six competing decay modes as (Z, h, γ) plus (\tilde{G}', \tilde{G}) , we are interested in a scenario where the neutralino predominantly decays into a pseudo-goldstino and a Z boson. This scenario can be realized by enhancing the coupling parameters \tilde{y} , especially \tilde{y}_{Z_T} and \tilde{y}_{Z_L} , and by assuming the Higgsino-like neutralino. The decay formulas are reported in Appendix A, where we also provide the details of our illustrative benchmark point in the SUSY breaking parameters determining the couplings \tilde{y} and y ; we typically take $\mu \sim 800$ GeV and $M_B = M_W \sim 1.5$ TeV. For the parameters we consider in this paper, the mass splitting between the two neutralinos is of the order of a few GeV. In this scenario, the second lightest neutralino $\tilde{\chi}_2^0$ decays to the lightest neutralino $\tilde{\chi}_1^0$ with soft SM particle emissions. Indeed we checked with SUSY-HIT [28] and the formula in Appendix A that its decay modes to the goldstino and to the pseudo-goldstino for our benchmark point are negligible compared with the $\tilde{\chi}_2^0 \rightarrow \tilde{\chi}_1^0$ decays. Hence in the following we assume $B(\tilde{\chi}_2^0 \rightarrow \tilde{\chi}_1^0 + \text{undetected SM particles}) = 100\%$. The final state topology is then determined by the possible $\tilde{\chi}_1^0$ decays, which we now investigate.

In Fig. 2 we show the branching ratios of the lightest neutralino as a function of the pseudo-goldstino mass, evaluated on our illustrative benchmark point described in detail in Appendix A. The decay pattern depends on the mass splitting $\Delta m_{\tilde{\chi}_1^0 - \tilde{G}'} \equiv m_{\tilde{\chi}_1^0} - m_{\tilde{G}'}$, and on the possible kinematically allowed modes. The branching ratio of $\tilde{\chi}_1^0 \rightarrow Z\tilde{G}'$ is always greater than 80% for $\Delta m_{\tilde{\chi}_1^0 - \tilde{G}'} > m_h$, and saturates at 100% for $m_Z < \Delta m_{\tilde{\chi}_1^0 - \tilde{G}'} < m_h$. We note that the $\tilde{\chi}_1^0 \rightarrow \gamma\tilde{G}'$ decay is negligible in our parameter choice. In the regime of $\Delta m_{\tilde{\chi}_1^0 - \tilde{G}'} < m_Z$, the decays into a true goldstino plus a γ , Z or h become dominant due to the phase space. In the following, we consider the region

$$\Delta m_{\tilde{\chi}_1^0 - \tilde{G}'} > m_Z, \quad (5)$$

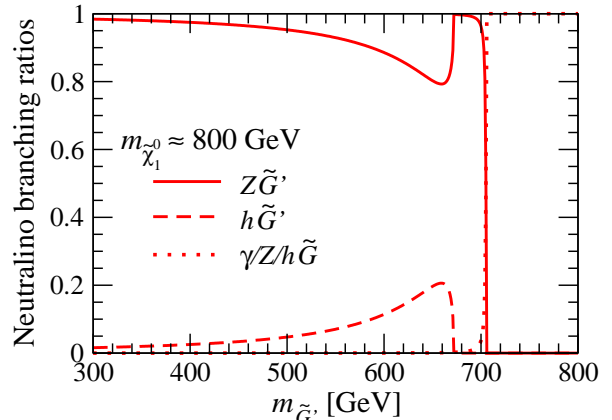


Figure 2: Branching ratios of the lightest neutralino as a function of the pseudo-goldstino mass for a representative benchmark point given in Appendix A. The $\tilde{\chi}_1^0 \rightarrow \gamma\tilde{G}'$ decay is too small to see in the plot.

where the $\tilde{\chi}_1^0 \rightarrow Z\tilde{G}'$ decay is dominant, as assumed in the simplified model in Fig. 1 and shown in Fig. 2.

We have also verified that the total decay width in the region of interest is always larger than 2×10^{-12} GeV, implying that the decays happen promptly in the detector.

Finally, the pseudo-goldstino will eventually decay into a goldstino plus γ , Z or h . However, one can verify that the pseudo-goldstino is enough long-lived so that the decay happens outside the detector. With the formulas listed in Appendix A, one can indeed compute the pseudo-goldstino decay width and we find that for the benchmark point it is around $10^{-22} - 10^{-24}$ GeV, i.e. $\tau_{\tilde{G}'} \lesssim 1$ sec, depending on the pseudo-goldstino mass. Even though we are not addressing cosmological issues in this paper, we observe that this decay is fast enough not to spoil the big bang nucleosynthesis (BBN) [29].

3. Analyses

At the LHC, our simplified goldstini model can be probed by gluino production. Given the discussion on the decays in the previous section, the gluino pair production leads to the process illustrated in Fig. 3, where we assume the 100% branching ratio at each decay step as a good approximation. Depending on the decay of the Z boson, the final state can be SFOS lepton pair + jets + \cancel{E}_T and jets + \cancel{E}_T .

In this section, we investigate whether or not the event topology of our model can successfully fit the ATLAS on- Z excess without conflicting with other searches. The most stringent constraints come from ATLAS multijet search [15] and CMS dilepton search [16] in the parameter region of our interest [3, 4, 8]. The latter has signal regions which look at the same final state as in the ATLAS on- Z signal region and potentially quite constraining. We have implemented these analyses as well as the ATLAS on- Z signal region in **Atom** [30]. Some description and validation results of **Atom** are given in Appendix B.

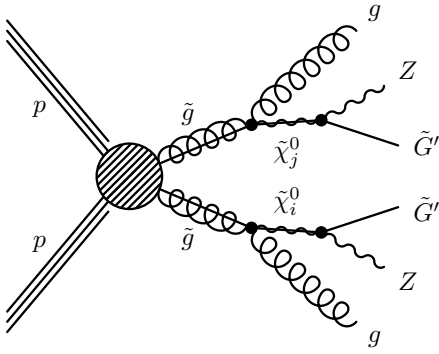


Figure 3: The process at the LHC in our simplified goldstini model.

In order to fit the excess we scan the gluino mass having the neutralino masses fixed at

$$m_{\tilde{\chi}_{1,2}^0} = m_{\tilde{g}} - 200 \text{ GeV}. \quad (6)$$

We consider three cases featuring the pseudo-goldstino mass:

$$m_{\tilde{G}'} = \begin{cases} 0 & \text{(A)} \\ m_{\tilde{\chi}_i^0} - 200 \text{ GeV} & \text{(B)} \\ m_{\tilde{\chi}_i^0} - 100 \text{ GeV} & \text{(C)} \end{cases} \quad (7)$$

Case A is equivalent to the gauge mediation scenario with only one SUSY breaking sector and a very light gravitino, while cases B and C have compressed spectra.

In order to assess the consistency between the model and data, the ideal approach would be to carry out a global fit, treating the excess and constraints in the same manner. This requires the details of the systematic uncertainties and good understanding of the correlation among different signal regions. Rather than taking this rigorous approach, in this exploratory paper we instead fit the model to the excess independently from the constraints and check the exclusion individually for the signal regions using the following prescription.

To see a goodness of the fit, we define the measure R as

$$R \equiv N_{\text{SUSY}} / (N_{\text{obs}} - N_{\text{SM}}), \quad (8)$$

for the ATLAS on- Z signal region, where N_{SUSY} is the expected SUSY events, N_{obs} is the number of observed events and N_{SM} is the expected SM events in the signal region. With this definition the best fit is given at $R = 1$.

For the other signal regions, labeled i , used as constraint, we instead define

$$R^i \equiv N_{\text{SUSY}}^i / N_{\text{BSM}}^{\text{UL},i}, \quad (9)$$

where N_{SUSY}^i is the expected SUSY events and $N_{\text{BSM}}^{\text{UL},i}$ is the 95% CL_s limit obtained from signal region i . Having any R_i greater than one indicates that the model is strongly disfavoured.

The $N_{\text{SUSY}}^{(i)}$ can be expressed as $\sigma_{\tilde{g}\tilde{g}} \cdot \mathcal{L} \cdot \epsilon_{(i)}$. Here \mathcal{L} is the integrated luminosity used in the analysis and $\sigma_{\tilde{g}\tilde{g}}$ is the production cross section of the gluino pair, for which we use the values reported in [31, 32]. To estimate the efficiency $\epsilon_{(i)}$ we use the following simulation chain: first the signal events are generated using MadGraph5_aMC@NLO [33] and showered and hadronized by Pythia6 [34]. The hadron level events are then passed to Atom [30] to estimate the efficiency for each signal region taking the detector effects into account. For our signal simulation, we extended the goldstini model [21, 35] (building on [36]) to include the two-body gluino decay by using FeynRules2 [37].

The results of the three cases of the goldstini scenario in Eq. (7) are presented in Figs. 4 and 5, where the modes are confronted with the ATLAS multijet [15] and the CMS dilepton [16] searches, respectively. The fitting measure R for the ATLAS on- Z signal region [1] is shown with the solid black curve, whereas the constraints R^i are shown with the other curves, corresponding to the signal regions (2jl, 2jm, 2jt, 3j, 4jl-, 4jl, 4jm, 4jt, 5j, 6j, 6jm, 6jt, 6j+) in the ATLAS multijet search in Fig. 4 and (cms2jl, cms2jm, cms2jh, cms3jl, cms3jm, cms3jh, cms(C), cms(F)) in the CMS dilepton search in Fig. 5.¹ The green (yellow) band around $R = 1$ represents the 1 (2) σ region of the fit for the ATLAS on- Z excess.

One can see that the entire region of case A, i.e. the massless goldstino case, is excluded by the ATLAS multijet search. The CMS dilepton search also excludes the region with $m_{\tilde{g}} < 1.1$ TeV. These strong limits can be attributed to the large mass gap between the gluino and the pseudo-goldstino, because of which the jets and leptons from the gluino decays tend to be hard, helping to increase the efficiency of the ATLAS multijet search as well as the CMS dilepton search.

Moving to case B and C, one can see that the constraints are generally more relaxed than in case A, since these cases have milder mass hierarchy with the massive pseudo-goldstino. The ATLAS multijet search now excludes the gluino mass up to 970 (810) GeV for case B (C). Here, the best fit of the ATLAS on- Z excess is given at $m_{\tilde{g}} = 980$ (900) GeV for case B (C), which is just outside of the ATLAS multijet exclusion limit.

The CMS dilepton search, on the other hand, still provides tight constraints, especially the cms2jh signal region, where $\cancel{E}_T > 300$ GeV is required, very similar to the $\cancel{E}_T > 225$ GeV cut in the ATLAS on- Z analysis. The difference between the two analyses is that the ATLAS search additionally imposes $H_T > 600$ GeV, where H_T is the scalar sum of the p_T of jets and leptons. For case B, the best fit point ($m_{\tilde{g}} = 980$ GeV) is just on the

¹ The n_j in the signal region name indicates it requires more than n high p_T jets. The letter “l”, “m”, “t” for the ATLAS multijet search means “loose”, “medium”, “tight”, while “l”, “m”, “h” for the CMS dilepton search denotes “low”, “medium”, “high”. The cms(C) and cms(F) represent the central and forward signal regions in which the number of jets and \cancel{E}_T are treated inclusively. See [15] and [16] for the exact definition.

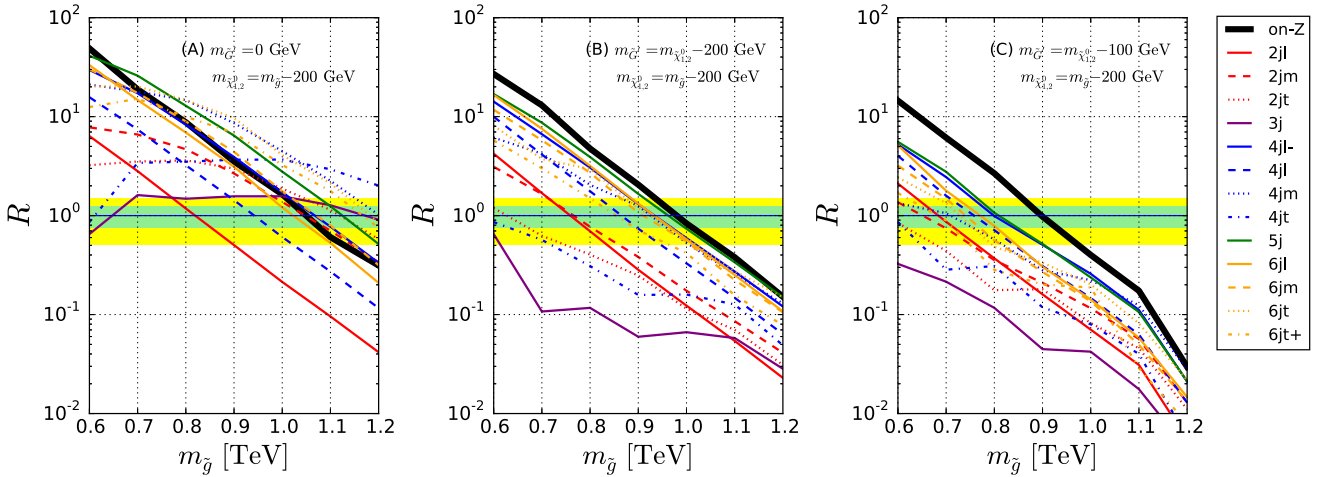


Figure 4: R values for the fit (black solid) and constraints (others) for cases A (left), B (middle) and C (right) in Eq. (7). The green and yellow bands correspond to the 1 and 2 σ regions of the fit. If the black curve is in the bands, the model provides a good fit for the ATLAS on- Z excess [1]. On the other hand, if there is any other curve above one, the model point is strongly disfavoured by the signal region corresponding to the curve in the ATLAS multijet + \cancel{E}_T analyses [15].

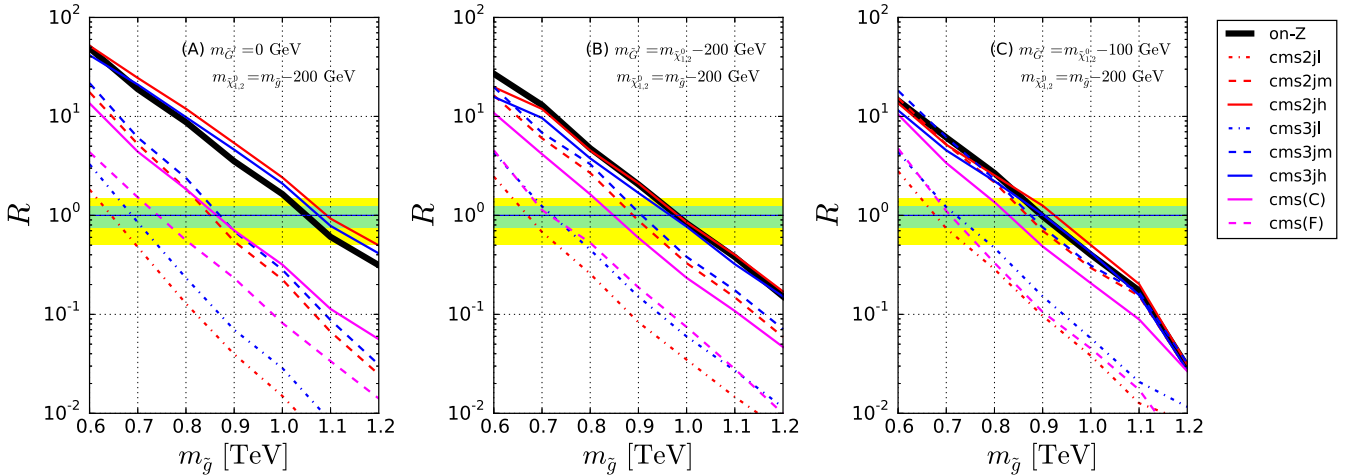


Figure 5: The same as in Fig. 4, but for the constraints from the CMS on- Z analyses [16].

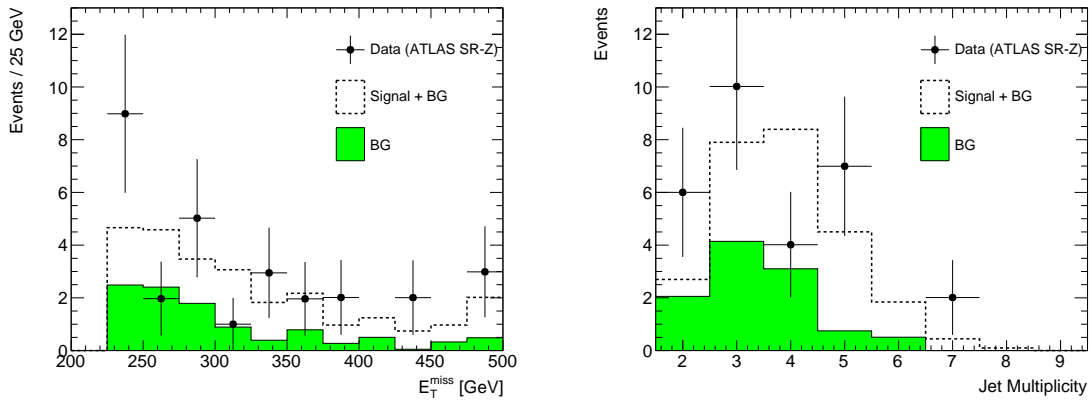


Figure 6: Comparison between data and signal + background in the \cancel{E}_T (left) and jet multiplicity (right) distributions in the ATLAS on- Z signal region [1] at our best fit point: $(m_{\tilde{g}}, m_{\tilde{\chi}_{1,2}^0}, m_{\tilde{G}'}) = (1000, 800, 600)$ GeV.

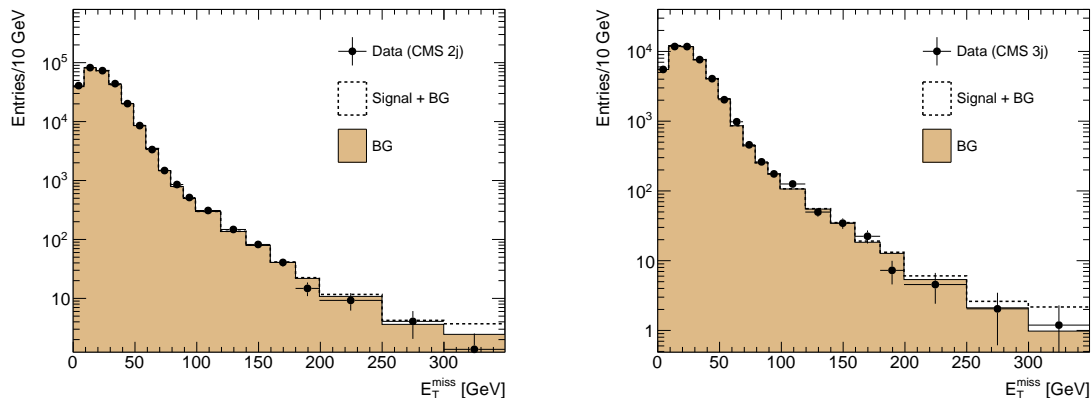


Figure 7: Comparison between data and signal + background in the \cancel{E}_T distribution in the CMS on- Z signal region with ≥ 2 jets (left) and ≥ 3 jets (right) [16] at our best fit point: $(m_{\tilde{g}}, m_{\tilde{\chi}_{1,2}^0}, m_{\tilde{G}'}) = (1000, 800, 600)$ GeV.

exclusion boundary, while for case C the best fit point ($m_{\tilde{g}} = 900$ GeV) is just excluded by the cms2jh signal region. For case B, at $m_{\tilde{g}} = 1$ TeV, the fit for the ATLAS on- Z excess is still within the 1σ band, and the point is still outside of the 95% CL_s exclusion. We therefore choose our best fit benchmark point as

$$(m_{\tilde{g}}, m_{\tilde{\chi}_{1,2}^0}, m_{\tilde{G}'}) = (1000, 800, 600) \text{ GeV} \quad (10)$$

for the following analysis. Even for case C, the tension between the data and the prediction observed in the ATLAS on- Z signal region can be ameliorated to the 2σ level with $m_{\tilde{g}} = 950$ GeV, which is outside the 95% CL_s exclusion region.

In Fig. 6 we compare the data with the signal + background in the \cancel{E}_T (left) and jet multiplicity (right) distributions in the ATLAS on- Z signal region at our best fit point in (10). Here we took the data and the SM background from Figs. 6 and 7 in the ATLAS paper [1] and combined ee and $\mu\mu$ channels. The data in the \cancel{E}_T distribution has a preference of low \cancel{E}_T , peaking around 240 GeV and roughly falling down up to around 500 GeV. The distribution is well fitted with the signal + background at our best fit point because the massive nature of the pseudo-goldstino reduces the \cancel{E}_T in the event. In the jet multiplicity distribution the data prefers 2 – 5 jets and disfavors the region with ≥ 6 jets. The distribution of the signal + background at our best fit point peaks around 3 – 4 and gives a good fit to the data. This is an advantage of the radiative decay $\tilde{g} \rightarrow g\tilde{\chi}_{1,2}^0$ compared to the three-body $\tilde{g} \rightarrow q\bar{q}\tilde{\chi}_{1,2}^0$ decay because the number of jets is reduced typically by two.

As a reference, in Fig. 7 we also compare the signal with the CMS data in the on- Z signal region with $N_{\text{jets}} \geq 2$ and ≥ 3 at our best fit point in (10). Here we took the data and the SM background from Fig. 7 in the CMS paper [16]. As already seen in Fig. 5, the most stringent constraint comes from the high \cancel{E}_T region, i.e. cms2jh and cms3jh, where the $\cancel{E}_T > 300$ GeV bin is considered.

4. Summary

Even though LHC at 8 TeV has not discovered a new physics signal, the Run-I data contain a few small excesses that deserve a thorough investigation. Recently the ATLAS Collaboration has reported a 3.0σ excess in dilepton + jets + \cancel{E}_T , with the dilepton reconstructing the Z -boson mass.

In this paper we have proposed an explanation of such excess in a SUSY model of gauge mediation with two SUSY breaking sectors, presenting in the SUSY spectrum an extra neutral fermion besides the MSSM neutralinos, that is the pseudo-goldstino. Our simplified model consists in a gluino, a pair of Higgsino-like neutralinos, and a pseudo-goldstino. We showed that our goldstini model can explain the ATLAS Z -peaked excess without conflicting with the constraints from multijet + \cancel{E}_T as well as from the CMS analysis for the same final state. The compressed spectrum such as $m_{\tilde{g}} \sim 1000$ GeV, $m_{\tilde{\chi}_{1,2}^0} \sim 800$ GeV and $m_{\tilde{G}'} \sim 600$ GeV gives a very good fit to the data not only for the rate but also for the distributions.

If this is indeed the origin of the excess, the 13-TeV LHC with both the ATLAS and CMS Collaborations will soon confirm the excess with much greater significance. We await the verdict from the LHC Run-II.

Acknowledgments

We would like to thank Gabriele Ferretti, Diego Redigolo, and Pantelis Tziveloglou for helpful discussions, and Satoshi Shirai for valuable comments on the cosmological issue. We are particularly grateful to Yevgeny Kats for useful suggestion on the CMS constraints.

S.P.L. is supported by JSPS Research Fellowships for Young Scientists and the Program for Leading Graduate Schools, MEXT, Japan. A. M. is a Pegasus FWO post-doctoral Fellowship. K.S. is supported in part by the London Centre for Terauniverse Studies (LCTS), using fund-

ing from the European Research Council via the Advanced Investigator Grant 267352. M.V. is an aspirant FWO-Vlaanderen. K.M., A. M. and M.V. are also supported in part by the Strategic Research Program High Energy Physics and the Research Council of the Vrije Universiteit Brussel.

Appendix A. Neutralino decay

In this appendix, we review the true goldstino and the pseudo-goldstino couplings with the MSSM states, and derive the formulas for the relevant decay widths; see also Refs. [11, 19, 21–23].

In the two-sector goldstini model, the lagrangian relevant to the neutralino decay, in the gauge eigenstate ($\tilde{\psi}_i = \{\tilde{B}, \tilde{W}, \tilde{H}_d, \tilde{H}_u\}$), is²

$$\mathcal{L} \supset -\frac{1}{2}M_{ij}^{\tilde{\psi}}\tilde{\psi}_i\tilde{\psi}_j - \rho_{ai}\tilde{G}_a\chi_i - \frac{1}{2}M_{ab}^{\tilde{G}}\tilde{G}_a\tilde{G}_b - \frac{1}{2}Y_{ij}\tilde{\psi}_i\tilde{\psi}_j h_0 + \tau_{ai}\tilde{G}_a\tilde{\psi}_i h_0 + G_{ij}\tilde{\psi}_i^\dagger\tilde{\sigma}^\mu\tilde{\psi}_j Z_\mu + iL_{ia}\tilde{\psi}_i\sigma^\mu\tilde{\sigma}^\nu\tilde{G}_a Z_{\mu\nu}, \quad (\text{A.1})$$

where $M_{ij}^{\tilde{\psi}}$ is the standard 4×4 neutralino mass matrix. The other parameters are

$$\rho_a = -\frac{1}{\sqrt{2}f_a} \begin{pmatrix} M_{B(a)}\langle D_Y \rangle \\ M_{W(a)}\langle D_{T^3} \rangle \\ \sqrt{2}v(m_{H_d(a)}^2 c_\beta - B_{(a)}s_\beta) \\ \sqrt{2}v(m_{H_u(a)}^2 s_\beta - B_{(a)}c_\beta) \end{pmatrix}, \quad (\text{A.2})$$

$$Y = \frac{1}{2} \begin{pmatrix} 0 & 0 & -g_1 c_\beta & g_1 s_\beta \\ 0 & 0 & g_2 c_\beta & -g_2 s_\beta \\ -g_1 c_\beta & g_2 c_\beta & 0 & 0 \\ g_1 s_\beta & -g_2 s_\beta & 0 & 0 \end{pmatrix}, \quad (\text{A.3})$$

$$\tau_a = \frac{1}{\sqrt{2}f_a} \begin{pmatrix} m_Z M_{B(a)} s_W c_2\beta \\ -m_Z M_{W(a)} c_W c_2\beta \\ m_{H_d(a)}^2 c_\beta - B_{(a)} s_\beta \\ m_{H_u(a)}^2 s_\beta - B_{(a)} c_\beta \end{pmatrix}, \quad (\text{A.4})$$

$$G = \frac{g_2}{2c_W} \begin{pmatrix} 0 & 0 & 0 & 0 \\ 0 & 0 & 0 & 0 \\ 0 & 0 & 1 & 0 \\ 0 & 0 & 0 & -1 \end{pmatrix}, \quad (\text{A.5})$$

$$L_a = \frac{1}{2\sqrt{2}f_a} \begin{pmatrix} -M_{B(a)} s_W \\ M_{W(a)} c_W \\ 0 \\ 0 \end{pmatrix}, \quad (\text{A.6})$$

where we denote with $M_{B/W(a)}$, $m_{H_d/u(a)}^2$ and $B_{(a)}$ the contribution to the soft term from sector a , and consider the decoupling limit for the Higgses. For convenience it is also useful to define tilded soft masses, e.g.

$$\tilde{M}_B = -\frac{f_2}{f_1}M_{B(1)} + \frac{f_1}{f_2}M_{B(2)}, \quad (\text{A.7})$$

while the non-tilded are the physical ones, e.g.

$$M_B = M_{B(1)} + M_{B(2)}. \quad (\text{A.8})$$

The mass matrix $M^{\tilde{G}}$ is

$$M^{\tilde{G}} = \begin{pmatrix} -\frac{f_2}{f_1}\mathcal{M}_{12} & \mathcal{M}_{12} \\ \mathcal{M}_{12} & -\frac{f_1}{f_2}\mathcal{M}_{12} \end{pmatrix}, \quad (\text{A.9})$$

and it is such that it has one zero eigenvalue along the true goldstino eigenstate in Eq. (2). The entry \mathcal{M}_{12} is a model dependent quantity that has been computed in [14]. The other eigenvalue of $M^{\tilde{G}}$ is the pseudo-goldstino mass $m_{\tilde{G}'}$.

Given a set of soft terms and the relative contributions from the two sectors, one should diagonalize the lagrangian and write the resulting couplings in the mass eigenbasis. This ends up in the lagrangian quoted in Eq. (4), whose couplings can be computed for a given set of soft terms. Note that, even though suppressed by $1/f_a$, there will be some mixing between the neutralinos and the goldstini. This is the reason why we have also written in (A.1) the terms containing only the neutralino gauge eigenstates. For instance, once rotated into the mass eigenbasis, these interactions generate the effective couplings \tilde{y}_{Z_L} in Eq. (4).

Although we study a rather heavy pseudo-goldstino case in this paper, we consider the $m_{\tilde{G}'} = 0$ limit for a while to get an insight on the feature of the pseudo-goldstino couplings by the analytic expressions. At leading order in $m_Z/m_{\tilde{\chi}}$ in the neutralino and pseudo-goldstino mixing and neglecting the pseudo-goldstino mass, the effective couplings in the pseudo-goldstino lagrangian (4) are

$$\tilde{y}_\gamma^i = m_{\tilde{\chi}_i^0} (K_B N_{i1} c_W + K_W N_{i2} s_W) + m_Z (N_{i4}^* s_\beta - N_{i3}^* c_\beta) s_W c_W (K_B - K_W), \quad (\text{A.10})$$

$$\tilde{y}_{Z_T}^i = m_{\tilde{\chi}_i^0} (-K_B N_{i1} s_W + K_W N_{i2} c_W) + m_Z (N_{i4}^* s_\beta - N_{i3}^* c_\beta) (s_W^2 K_B + c_W^2 K_W), \quad (\text{A.11})$$

$$\tilde{y}_{Z_L}^i = -m_Z K_\mu (-N_{i1} s_W + N_{i2} c_W) - m_{\tilde{\chi}_i^0} (K_u N_{i4}^* s_\beta - K_d N_{i3}^* c_\beta), \quad (\text{A.12})$$

$$\tilde{y}_h^i = -m_Z \cos 2\beta (-K_B M_B N_{i1}^* s_W + K_W M_W N_{i2}^* c_W) - \mu^2 (K_d N_{i3}^* c_\beta + K_u N_{i4}^* s_\beta), \quad (\text{A.13})$$

where the neutralino rotation matrix N_{ij} is defined as in [38]. The K factors read

$$K_B = \frac{\tilde{M}_B}{M_B}, \quad K_W = \frac{\tilde{M}_W}{M_W}, \quad K_\mu = c_\beta^2 K_d + s_\beta^2 K_u, \\ K_d = -\frac{1}{\mu^2} (\tilde{m}_{H_d}^2 - \tilde{B} \tan \beta + \frac{m_Z^2}{2} (s_W^2 K_B + c_W^2 K_W) \cos 2\beta), \\ K_u = -\frac{1}{\mu^2} (\tilde{m}_{H_u}^2 - \tilde{B} \cot \beta - \frac{m_Z^2}{2} (s_W^2 K_B + c_W^2 K_W) \cos 2\beta), \quad (\text{A.14})$$

²We follow the conventions of [38].

where we keep the terms of order m_Z^2 in the last two K factors in order to show the goldstino limit explicitly. The goldstino lagrangian [38–42] is recovered by converting all the tilded soft terms to the un-tilded ones, and using the electroweak symmetry breaking (EWSB) conditions

$$0 = m_{H_u}^2 + \mu^2 - B \cot \beta - \frac{1}{2} m_Z^2 \cos 2\beta, \quad (\text{A.15})$$

$$0 = m_{H_d}^2 + \mu^2 - B \tan \beta + \frac{1}{2} m_Z^2 \cos 2\beta, \quad (\text{A.16})$$

resulting in all the K factors in Eq. (A.14) to be unity. From the above analytic couplings, for instance, one can observe that for a mostly Higgsino-like neutralino with $K_B = K_W$ the pseudo-goldstino coupling to the photon is suppressed. We also checked that the above expressions agree with the numerics if the pseudo-goldstino mass is sufficiently smaller than the neutralino masses. For the large pseudo-goldstino mass, on the other hand, there can be deviations from these formulas once we rotate in the mass eigenbasis. Hence, in order to compute correctly the effective couplings in Eq. (4) for generic pseudo-goldstino masses, one is instructed to diagonalize numerically the lagrangian (A.1), for a given set of soft terms, and write it in the mass eigenbasis.

Once the effective couplings in Eq. (4) are evaluated, the neutralino decay widths can be computed as [19, 21]

$$\Gamma_{\tilde{\chi}_i^0 \rightarrow \gamma \tilde{G}'} = \frac{(\tilde{y}_\gamma^i)^2 m_{\tilde{\chi}_i^0}^3}{16\pi F^2} \left(1 - \frac{m_{\tilde{G}'}^2}{m_{\tilde{\chi}_i^0}^2}\right)^3, \quad (\text{A.17})$$

$$\begin{aligned} \Gamma_{\tilde{\chi}_i^0 \rightarrow Z \tilde{G}'} &= \frac{\beta_Z m_{\tilde{\chi}_i^0}}{32\pi F^2} \left[\left(1 - \frac{m_{\tilde{G}'}^2}{m_{\tilde{\chi}_i^0}^2}\right)^2 - \frac{m_Z^2}{m_{\tilde{\chi}_i^0}^2} \right] \\ &\times [(\tilde{y}_{Z_T}^i)^2 (2(m_{\tilde{\chi}_i^0} + m_{\tilde{G}'}^2)^2 + m_Z^2) \\ &+ (\tilde{y}_{Z_L}^i)^2 ((m_{\tilde{\chi}_i^0} + m_{\tilde{G}'}^2)^2 + 2m_Z^2) \\ &+ 6\tilde{y}_{Z_T}^i \tilde{y}_{Z_L}^i m_Z (m_{\tilde{\chi}_i^0} + m_{\tilde{G}'}^2)], \quad (\text{A.18}) \end{aligned}$$

$$\Gamma_{\tilde{\chi}_i^0 \rightarrow h \tilde{G}'} = \frac{\beta_h (\tilde{y}_h^i)^2 m_{\tilde{\chi}_i^0}^3}{32\pi F^2} \left(1 + 3 \frac{m_{\tilde{G}'}^2}{m_{\tilde{\chi}_i^0}^2} - \frac{m_h^2}{m_{\tilde{\chi}_i^0}^2}\right), \quad (\text{A.19})$$

where $\beta_{Z/h} = \bar{\beta}(m_{\tilde{G}'}^2/m_{\tilde{\chi}_i^0}^2, m_Z^2/m_{\tilde{\chi}_i^0}^2)$ with $\bar{\beta}(a, b) = (1 + a^2 + b^2 - 2a - 2b - 2ab)^{1/2}$. The standard decays into the massless goldstino are obtained from this expression by sending the tilded quantities to the non-tilded quantities and putting $m_{\tilde{G}'} \rightarrow 0$.

In this paper we are interested in configurations where the two lightest neutralinos are mostly Higgsinos and the decay of $\tilde{\chi}_1^0$ is predominantly into a massive pseudo-goldstino and a Z boson. To find if this scenario is compatible with the lagrangian just explained, we numerically explored the parameters of the model (i.e. the soft terms) looking for a representative benchmark point satisfying these requirements. In Fig. 2 we report the branching ratios for a configuration with $\mu = 804$ GeV, $\sqrt{B} = 800$ GeV, $M_B = M_W = 1.5$ TeV and $\tan \beta = 10$. The total soft masses for the Higgses are extracted by solving the EWSB conditions.

The two SUSY breaking scales are chosen as $\sqrt{f_1} = 1.5 \times 10^6$ GeV and $\sqrt{f_2} = 5 \times 10^4$ GeV. The gaugino masses and the Higgs soft masses are distributed in the two sectors as $M_{B/W(1)}/M_{B/W(2)} = \tan^2 \theta$, $m_{H_{d/u}(1)}^2/m_{H_{d/u}(2)}^2 = \cot^2 \theta$. The angle θ is taken to be $\tan \theta = 0.2$. Finally the B terms are chosen as $B_{(a)} = f_a/(f_1 + f_2)B$. With these values we obtain a scenario where the two lightest neutralinos are mostly Higgsinos, with masses at (797, 805) GeV. The lightest neutralino decay is predominantly into a pseudo-goldstino plus a Z boson for different ranges of pseudo-goldstino mass, as we show in Fig. 2. The pseudo-goldstino mass is varied by changing \mathcal{M}_{12} consistently with the perturbative definition in [14]. The decay width of the neutralinos cited in the text are computed with the decay formulas (A.17), (A.18) and (A.19). Moreover, the decay of the pseudo-goldstino can be computed using the same formula quoted above, where the coupling between the pseudo-goldstino and the goldstino are extracted numerically from the original lagrangian once we switch to the mass eigenbasis.

Appendix B. Analysis implementation

For this paper, we implemented several ATLAS and CMS analyses in the `Atom` framework [30]. `Atom` is a program based on `Rivet` [43] and maps the truth level particles into the reconstructed objects such as isolated electrons and b -jets according to the detector performances reported by ATLAS and CMS. The validation and some application of the code can be found in [44–48].

In Table B.1 we show some of the validation results as an example. The numbers in the second column represent the expected signal events for each step of the cut used in the 5j signal region (SR) reported by the ATLAS multijet analysis [15], based on the $\tilde{q}_L \rightarrow q\tilde{\chi}_1^\pm \rightarrow qW^\pm\tilde{\chi}_1^0$ topology with $(m_{\tilde{q}}, m_{\tilde{\chi}_1^\pm}, m_{\tilde{\chi}_1^0}) = (665, 465, 265)$ GeV. The right column shows the ratios between the `Atom` and ATLAS results. One can see that these ratios are close to one within $\sim 20\%$ accuracy indicating a good agreement between the `Atom` and ATLAS simulations.

| 5j SR cuts | $N_{\text{SUSY}}^{\text{Exp}}$ | Atom/Exp |
|--|--------------------------------|----------|
| $\cancel{E}_T > 160, p_T^{j_{1(2)}} > 130(60)$ GeV | 317.3 | 1.17 |
| $p_T^{j_3} > 60$ GeV | 306.2 | 1.12 |
| $p_T^{j_4} > 60$ GeV | 247.6 | 1.04 |
| $p_T^{j_5} > 60$ GeV | 141.8 | 1.00 |
| $\Delta\phi(j_{1,2,3}, \cancel{E}_T) > 0.4$ | 118.6 | 1.01 |
| $\Delta\phi(j_{i>3} > 40 \text{ GeV}, \cancel{E}_T) > 0.2$ | 103.1 | 1.01 |
| $\cancel{E}_T/m_{\text{eff}}(N_j) > 0.2$ | 85.6 | 1.04 |
| $m_{\text{eff}}(\text{incl.}) > 1200$ GeV | 20.5 | 1.18 |

Table B.1: “5j” SR validation table for the implementation of the ATLAS multijet analysis in `Atom`. The decay chain for validation in consideration is $\tilde{q}_L \rightarrow q\tilde{\chi}_1^\pm \rightarrow qW^\pm\tilde{\chi}_1^0$.

References

- [1] ATLAS Collaboration, G. Aad *et. al.*, *Search for supersymmetry in events containing a same-flavour opposite-sign dilepton pair, jets, and large missing transverse momentum in $\sqrt{s} = 8$ TeV pp collisions with the ATLAS detector*, *Eur. Phys. J.* **C75** (2015), no. 7 318, [1503.03290].
- [2] G. Barenboim, J. Bernabeu, V. Mitsou, E. Romero, E. Torro, *et. al.*, *METing SUSY on the Z peak*, 1503.04184.
- [3] U. Ellwanger, *Possible explanation of excess events in the search for jets, missing transverse momentum and a Z boson in pp collisions*, *Eur. Phys. J.* **C75** (2015), no. 8 367, [1504.02244].
- [4] B. Allanach, A. Raklev, and A. Kvellestad, *Consistency of the recent ATLAS Z + E_T^{miss} excess in a simplified GGM model*, *Phys.Rev.* **D91** (2015) 095016, [1504.02752].
- [5] J. Cao, L. Shang, J. M. Yang, and Y. Zhang, *Explanation of the ATLAS Z-Peaked Excess in the NMSSM*, *JHEP* **06** (2015) 152, [1504.07869].
- [6] A. Kobakhidze, A. Saavedra, L. Wu, and J. M. Yang, *ATLAS Z-peaked excess in MSSM with a light sbottom or stop*, 1504.04390.
- [7] M. Cahill-Rowley, J. Hewett, A. Ismail, and T. Rizzo, *The ATLAS Z + MET Excess in the MSSM*, 1506.05799.
- [8] X. Lu, S. Shirai, and T. Terada, *ATLAS Z Excess in Minimal Supersymmetric Standard Model*, 1506.07161.
- [9] N. Vignaroli, *Z-peaked excess from heavy gluon decays to vector-like quarks*, *Phys.Rev.* **D91** (2015), no. 11 115009, [1504.01768].
- [10] B. A. Dobrescu, *Leptophobic boson signals with leptons, jets and missing energy*, 1506.04435.
- [11] C. Cheung, Y. Nomura, and J. Thaler, *Goldstini*, *JHEP* **1003** (2010) 073, [1002.1967].
- [12] K. Benakli and C. Moura, *Brane-Worlds Pseudo-Goldstinos*, *Nucl.Phys.* **B791** (2008) 125–163, [0706.3127].
- [13] C. Cheung, J. Mardon, Y. Nomura, and J. Thaler, *A Definitive Signal of Multiple Supersymmetry Breaking*, *JHEP* **1007** (2010) 035, [1004.4637].
- [14] R. Argurio, Z. Komargodski, and A. Mariotti, *Pseudo-Goldstini in Field Theory*, *Phys.Rev.Lett.* **107** (2011) 061601, [1102.2386].
- [15] ATLAS Collaboration, G. Aad *et. al.*, *Search for squarks and gluinos with the ATLAS detector in final states with jets and missing transverse momentum using $\sqrt{s} = 8$ TeV proton–proton collision data*, *JHEP* **1409** (2014) 176, [1405.7875].
- [16] CMS Collaboration, V. Khachatryan *et. al.*, *Search for physics beyond the standard model in events with two leptons, jets, and missing transverse momentum in pp collisions at $\sqrt{s} = 8$ TeV*, *JHEP* **1504** (2015) 124, [1502.06031].
- [17] N. Craig, J. March-Russell, and M. McCullough, *The Goldstini Variations*, *JHEP* **1010** (2010) 095, [1007.1239].
- [18] H.-C. Cheng, W.-C. Huang, I. Low, and A. Menon, *Goldstini as the decaying dark matter*, *JHEP* **1103** (2011) 019, [1012.5300].
- [19] J. Thaler and Z. Thomas, *Goldstini Can Give the Higgs a Boost*, *JHEP* **1107** (2011) 060, [1103.1631].
- [20] C. Cheung, F. D’Eramo, and J. Thaler, *The Spectrum of Goldstini and Modulini*, *JHEP* **1108** (2011) 115, [1104.2600].
- [21] R. Argurio, K. De Causmaecker, G. Ferretti, A. Mariotti, K. Mawatari, *et. al.*, *Collider signatures of goldstini in gauge mediation*, *JHEP* **1206** (2012) 096, [1112.5058].
- [22] T. Liu, L. Wang, and J. M. Yang, *Higgs decay to goldstini and its observability at the LHC*, *Phys.Lett.* **B726** (2013) 228–233, [1301.5479].
- [23] G. Ferretti, A. Mariotti, K. Mawatari, and C. Petersson, *Multiphoton signatures of goldstini at the LHC*, *JHEP* **1404** (2014) 126, [1312.1698].
- [24] K.-i. Hikasa, T. Liu, L. Wang, and J. M. Yang, *Pseudo-goldstino and electroweak gauginos at the LHC*, *JHEP* **1407** (2014) 065, [1403.5731].
- [25] T. Liu, L. Wang, and J. M. Yang, *Pseudo-goldstino and electroweakinos via VBF processes at LHC*, *JHEP* **1502** (2015) 177, [1411.6105].
- [26] H. Baer, X. Tata, and J. Woodside, *Phenomenology of Gluino Decays via Loops and Top Quark Yukawa Coupling*, *Phys.Rev.* **D42** (1990) 1568–1576.
- [27] P. Gambino, G. Giudice, and P. Slavich, *Gluino decays in split supersymmetry*, *Nucl.Phys.* **B726** (2005) 35–52, [hep-ph/0506214].
- [28] A. Djouadi, M. Muhlleitner, and M. Spira, *Decays of supersymmetric particles: The Program SUSY-HIT (SUSpect-SdecaY-Hdecay-InTerface)*, *Acta Phys.Polon.* **B38** (2007) 635–644, [hep-ph/0609292].
- [29] M. Kawasaki, K. Kohri, and T. Moroi, *Big-Bang nucleosynthesis and hadronic decay of long-lived massive particles*, *Phys.Rev.* **D71** (2005) 083502, [astro-ph/0408426].
- [30] I.-W. Kim, M. Papucci, K. Sakurai, and A. Weiler, *ATOM: Automated Tests Of Models*, in preparation.
- [31] LHC SUSY Cross Section Working Group, <https://twiki.cern.ch/twiki/bin/view/lhcsphysics/susycrosssections>, .
- [32] M. Kramer, A. Kulesza, R. van der Leeuw, M. Mangano, S. Padhi, *et. al.*, *Supersymmetry production cross sections in pp collisions at $\sqrt{s} = 7$ TeV*, 1206.2892.
- [33] J. Alwall, R. Frederix, S. Frixione, V. Hirschi, F. Maltoni, *et. al.*, *The automated computation of tree-level and next-to-leading order differential cross sections, and their matching to parton shower simulations*, *JHEP* **1407** (2014) 079, [1405.0301].
- [34] T. Sjostrand, S. Mrenna, and P. Z. Skands, *PYTHIA 6.4 Physics and Manual*, *JHEP* **0605** (2006) 026, [hep-ph/0603175].
- [35] K. Mawatari, *Associated production of light gravitinos at future linear colliders*, 1202.0507.
- [36] K. Mawatari and Y. Takaesu, *HELAS and MadGraph with goldstinos*, *Eur.Phys.J.* **C71** (2011) 1640, [1101.1289].
- [37] A. Alloul, N. D. Christensen, C. Degrande, C. Duhr, and B. Fuks, *FeynRules 2.0 - A complete toolbox for tree-level phenomenology*, *Comput.Phys.Commun.* **185** (2014) 2250–2300, [1310.1921].
- [38] S. P. Martin, *A Supersymmetry primer*, *Adv.Ser.Direct.High Energy Phys.* **21** (2010) 1–153, [hep-ph/9709356].
- [39] S. Ambrosanio, G. L. Kane, G. D. Kribs, S. P. Martin, and S. Mrenna, *Search for supersymmetry with a light gravitino at the Fermilab Tevatron and CERN LEP colliders*, *Phys.Rev.* **D54** (1996) 5395–5411, [hep-ph/9605398].
- [40] Z. Komargodski and N. Seiberg, *From Linear SUSY to Constrained Superfields*, *JHEP* **0909** (2009) 066, [0907.2441].
- [41] F. Luo, K. A. Olive, and M. Peloso, *The Gravitino coupling to broken gauge theories applied to the MSSM*, *JHEP* **1010** (2010) 024, [1006.5570].
- [42] I. Antoniadis, E. Dudas, D. Ghilencea, and P. Tziveloglou, *Non-linear MSSM*, *Nucl.Phys.* **B841** (2010) 157–177, [1006.1662].
- [43] A. Buckley, J. Butterworth, L. Lonnblad, D. Grellscheid, H. Hoeth, *et. al.*, *Rivet user manual*, *Comput.Phys.Commun.* **184** (2013) 2803–2819, [1003.0694].
- [44] M. Papucci, J. T. Ruderman, and A. Weiler, *Natural SUSY Endures*, *JHEP* **1209** (2012) 035, [1110.6926].
- [45] M. Papucci, K. Sakurai, A. Weiler, and L. Zeune, *Fastlim: a fast LHC limit calculator*, *Eur.Phys.J.* **C74** (2014), no. 11 3163, [1402.0492].
- [46] J. S. Kim, K. Rolbiecki, K. Sakurai, and J. Tattersall, *‘Stop’ that ambulance! New physics at the LHC?*, *JHEP* **1412** (2014) 010, [1406.0858].
- [47] P. Grothaus, S. P. Liew, and K. Sakurai, *A closer look at a hint of SUSY at the 8 TeV LHC*, *JHEP* **1505** (2015) 133, [1502.05712].
- [48] T. Jacques and K. Nordström, *Mapping monojet constraints onto Simplified Dark Matter Models*, *JHEP* **06** (2015) 142, [1502.05721].